MOLECULAR DYNAMICS SIMULATION OF GAS ADSORPTION AND ABSORPTION IN NANOTUBES

CHAPTER · DECEMBER 2005

DOI: 10.1007/1-4020-4574-3_31

1 AUTHOR:

Ana Proykova

Sofia University "St. Kliment Ohridski"

90 PUBLICATIONS **468** CITATIONS

SEE PROFILE

MOLECULAR DYNAMICS SIMULATION OF GAS ADSORPTION AND ABSORPTION IN NANOTUBES

SIMULATIONS OF GAS ADSORPTION ON/IN NANOTUBES

ANA PROYKOVA
University of Sofia, Faculty of Physics, 5 J. Bourchier Blvd., Sofia-1126, Bulgaria

*To whom correspondence should be addressed.

Abstract-

Keywords: adsorption; simulations of carbon nanotubes; Molecular Dynamics method; coarse-graining technique; ab-initio calculations; time-scales

1. Adsorption – general characteristics

Adsorption of one or more of the components at one or more of the phase boundaries of a multicomponent, multiphase system is said to occur if the concentrations in the interfacial layers are different from those in the adjoining bulk phases, so that the overall stoichiometry of the system deviates from that corresponding to a *reference system* of homogeneous bulk phases whose volumes and/or amounts are defined by suitably chosen dividing surfaces or by a suitable algebraic method.

1.1. PHYSISORPTION AND CHEMISORPTION

A qualitative distinction is usually made between *chemisorption* and *physisorption*. The problem of distinguishing between chemisorption and physisorption is basically the same as that of distinguishing between chemical and physical interaction in general. No absolutely sharp distinction can be made and intermediate cases exist, for example, adsorption involving strong hydrogen bonds or weak charge transfer. In terms of the relative binding strengths and mechanisms, a strong 'chemical bond' is formed between the adsorbate atom or molecule and the substrate. In the case of chemisorption the adsorption energy, E_a, of the adatom is of a few eV/atom.

Journal Information

Physisorption (or *physical adsorption*) results from the presence of van der Waals attractive forces due to fluctuating dipole (and higher order) moments on the interacting adsorbate and substrate with no charge transfer or electrons shared between atoms. These intermolecular forces, usually between closed-shell systems, are of the same kind as those responsible for the imperfection of real gases and the condensation of vapours.

Table 1The following features characterize physisorption and chemisorption.

Physisorption	Chemisorption
Evidence for the perturbation of the electronic states of adsorbent and adsorbate is minimal	Changes in the electronic state
The chemical nature of the adsorptive is not altered by adsorption and subsequent desorption	The chemical nature of the adsorptive(s) may be altered, i.e. the chemisorption may not be reversible.
Energies are of order 50-500 meV/atom	The energy is of the same order of magnitude as the energy change in a chemical reaction between a solid and a fluid, eV/atom
The elementary step in physisorption from a gas phase does not involve activation energy	The elementary step in chemisorption often involves *activation energyi* (*adsorption sites*)
multilayer adsorption or filling of micropores	one layer of chemisorbed molecules is formed

Physisorption energies are of order 50-500 meV/atom. As they are small, they can be expressed in K/atom, via 1 eV ≡ 11604K, omitting Boltzmann's constant in the corresponding equations. One can see that these energies are comparable to the sublimation energies of rare gas solids.

The physical adsorption is believed to serve as a precursor, which enhances the transition to the chemisorption state. A first, *precursor* stage, has all the characteristics of physisorption, but this state is metastable. In this state the molecule may re-evaporate, or it may stay on the surface long enough to transform *irreversibly* into a chemisorbed state.

This transition from physisorption to chemisorption usually results in a split of the molecule and adsorption of individual atoms: *dissociative chemisorption*. If the heat of adsorption is given up suddenly and is imparted to the resulting adatoms, then the dissociation stage is explosive as it is in the case of F_2.The adsorption energies for the precursor phase are similar to phyisorption of rare gases, but may contain additional contributions from the dipole, quadrupole, or higher molecular multipoles..

1.2. LOCALIZED ADSORPTION AT LOW COVERAGE

Equilibrium phenomena are described by thermodynamics, which is the dynamics of heat or by statistical mechanics, which works well for large (on the order of Avogadro's number) numbers of particles – atoms and /or molecules. However, many properties of nanosized (small number of particles, away from the thermodynamics limit) materials are concerned with kinetics, where the rate of change of metastable structures (or their inability to change) is dominant (Proykova et al 2001, Proykova 2002). An equilibrium effect is the vapor pressure of a crystal (pure element). A kinetic effect is crystal growth from the vapor.

The *surface coverage* for both monolayer and multilayer adsorption is defined as the ratio of the amount of adsorbed substance to the ***monolayer capacity***. *For chemisorption* the monolayer capacity is defined as the amount of adsorbate, needed to occupy all adsorption sites as determined by the adsorbent structure and by the chemical nature of the adsorptive; *for physisorption* it is the amount needed to cover the surface with a complete monolayer of molecules in a close-packed array (Venables 2000).

The sublimation of a pure solid at equilibrium is given by the condition $\mu_v = \mu_s$, where μ_v is the chemical potential of the vapor and μ_s is the chemical potential of the solid. At low pressure p, μ_v is:

$$\mu_v = - kT \ln (kT/p\lambda^3),$$

where $\lambda = h/(2\pi mkT)^{1/2}$ is the thermal de Broglie wavelength; h is the Planck constant; k is the Boltzmann constant; m is the electron mass.

The equilibrium vapor pressure p_{eq} in terms of the chemical potential of the solid is

$$p_{eq} = (2\pi m/h^2)^{3/2} (kT)^{5/2} \exp (\mu_s /kT).$$

To calculate the vapor pressure we usually model μ_s at a low pressure assuming harmonic vibrations of the solid at a given lattice constant. The free energy per particle is

$$F/N = \mu_s = U_0 + <3h\nu/2> + 3kT<\ln(1-\exp(-h\nu/kT))>,$$

where < > denote averaged values. The (positive) sublimation energy at zero temperature is

$$L_0 = -(U_0 + <3h\nu/2>),$$

where the first term is the (negative) energy per particle in the solid relative to vapor, and the second is the (positive) energy due to zero-point vibrations.

The vapor pressure is important at high temperatures, where the Einstein model (all 3N ν's are the same) of the solid becomes realistic if thermal expansion is taken into account in U_0. This model gives

$$< \ln(1-\exp(-h\nu/kT))> = <\ln (h\nu/kT)>,$$

so that $\exp (\mu_s /kT) = (h\nu/kT)^3 \exp (-L_0/kT)$ and

$$p_{eq} = (2\pi m\nu^2)^{3/2} (kT)^{-1/2} \exp (-L_0 /kT).$$

Thus $p_{eq}T^{1/2}$ follows the Arrhenius law and the pre-exponential factor depends on the lattice vibration frequency as ν^3. The missing Planck's constant h shows a classical effect with equipartitioning of energy. Since the $T^{1/2}$ term slowly varies most tabulations of vapor pressure give the constants A and B from $\log_{10}(p_{eq}) = A - B/T$. The values for L_0 and ν are obtained along these lines.

The chemical potential μ_a of the adsorbed layer satisfies two possible conditions: $\mu_a = \mu_v$ for equilibrium with the vapor or $\mu_a = \mu_s$ for equilibrium with the solid.

The canonical partition function for the adsorbed atoms is $Z_a = \sum_i \exp (-E_i/kT)$ with $F = -kT\ln(Z)$. For N_a adsorbed atoms distributed over N_0 sites with the same adsorption energy E_a, $Z_a = Q(N_a,N_0) \exp (N_aE_a/kT)$, where Q is the configurational (and vibrational) degeneracy. The *configurational entropy* appears since, at low coverage, there are many ways to arrange the adatoms on the available adsorption sites, (Hill 1987): $Q = N_0!/(N_a !)(N_0-N_a)!$ multiplied by q^{Na} if vibrational effects are included. The expression for ln(Q) is evaluated using Stirling's approximation for $N! = N \ln(N) - N$ to give $\mu_a = F/N_a = -(kT/N_a) \ln (Z_a) = kT \ln (\theta/(1-\theta)) - E_a - kT \ln(q)$ and $\theta = N_a/N_0$. The first term is the configurational contribution in terms of the adatom coverage θ, the second term is the adsorption energy (measured positive with the vacuum level zero), and the last term is the (optional) vibrational contribution. The density of adatoms is determined by $\mu_s = 3kT \ln(h\nu/kT) - L_0 = \mu_a$ in the high temperature Einstein model. Thus at low coverage, θ is

$$\theta = N_a/N_0 = C\exp\{(-L_0 + E_a)/kT\},$$

where the pre-exponential function depends on vibrations in the solid, and the important exponential term depends on the difference between the sublimation and the adsorption energy. If C is unknown, we usually put it equal to 1 to obtain a first estimate of θ at a given temperature.

The *Langmuir Adsorption Isotherm* results from $\mu_a = \mu_v$. Using this to calculate the vapor pressure p in equilibrium with the adsorbed layer we get

$$p = C_1\theta/(1-\theta) \exp (-E_a/kT),$$

or $\theta = \xi(T)p/[1-\xi(T)p]$, with $\xi(T) = C_1^{-1}\exp(E_a/kT)$; the constant $C_1 = kT/q\lambda^3$. The coverage is linearly proportional to p for small p approaching 1 as $p \rightarrow \infty$.

The other limit of isolated adatom behaviour is the 2D gas (Venables 2000). This case is appropriate to a very smooth substrate, with shallow potential wells. The mobile adatoms see the *average adsorption energy* E_0, and gain additional entropy from the gaseous motion. The chemical potential is now $\mu_a = -E_0 + kT \ln(N_a\lambda^2/Aq_z)$, where this expression is valid at sufficiently low density for the distinction between classical Bose-Einstein and Fermi-Dirac statistics not to be important. The derivation involves evaluating the partition function by summing over 2D momenta, analogously to a 3D gas, while retaining the z-motion partition function q_z. **The 3D to 2D difference accounts for λ^2 rather than λ^3, and the N_a/A, the number of adsorbed atoms per unit area, is the 2D version of the 3D density N/V, as in pV = NkT.**

The perfect gas law has the 2D form $\Phi A = N_a kT$, where Φ is the *spreading pressure* (Venables 2000). This means that $\mu_a = -E_0 + kT \ln(\Phi\lambda^2/kT)$, or $\mu_a = -E_0 + \mu_2 + kT \ln(\Phi)$, where $\mu_2 = -kT \ln (kTq_z/\lambda^2)$ is the standard free energy for the 2D gas. This makes the correspondence between 3D gases and 2D adsorption clear: $p \leftrightarrow \Phi$, $\mu_0 \leftrightarrow \mu_2$; the energy is lower in the 2D case by E_0. The various q's are dimensionless and often skipped.

The *Henry's Law* for 2D gas adsorption is obtained by putting $\mu_a = \mu_v$:

$$p = C_2 (N_a/A) \exp (-E_0/kT),$$

or $(N_a/A) = \chi'(T)p$, with $\chi'(T) = C_2^{-1}\exp (E_0/kT)$, and $C_2 = kT/q_z\lambda$.

The 2D gas form has (N_a/A) proportional to p, whereas the localized form has the coverage $\theta = N_a/N_0$ proportional to p. These could be reconciled if we write $(N_a/A) = \theta (N_0/A)$. The monolayer coverage (N_0/A) and the area density of adsorbed atoms (N_a/A) have been defined as constants. Both N_0 and N_a are numbers, not area densities, although they are densities for A = 1. One can re-write the 2D gas equation as

$$p = (kTN_0/Aq_z\lambda)\, \theta \exp (-E_0/kT),$$

which is in a form that can be compared directly with the corresponding equation for localized adsorption. This comparison shows that there is a transition from localized to 2D gas-like behaviour as T is raised, because $E_a > E_0$, whereas the pre-exponential (entropic) term is larger for the 2D gas. The ratio of coverages at a given p for the two states is

$$(\theta_{gas}/\theta_{loc}) = (2\pi mkT/h^2 q_x q_y)(A/N_0) \exp[(E_0-E_a)/kT] =$$

$$= (2\pi ma^2\nu_d^2/kT) \exp[(E_0-E_a)/kT],$$

where the length *a* is an atomic dimension ($a^2 = A/N_0$), and the last equality is only true for the high temperature limit where equipartition of energy holds (no

term in h). We can state that the localized atoms will vibrate with an amplitude $\Re$ and $4\pi^2 m\Re^2\nu_d^2$ is the energy associated with this 2D oscillation, which equals 2kT at high T, assuming a harmonic approximation is valid. Thus, the pre-exponential is just a ratio of *free areas* ($a^2/\pi\Re^2$), the numerator associated with the 2D gas, and the denominator with the potential well in which the adatom vibrates. This is the basis of *cell models* of lattice vibrations, introduced originally by Lennard-Jones and Devonshire in 1937 (Hill 1986). The free area is defined by integrating the Boltzmann factor over the 'cell' in which the atom vibrates; in 3D this produces a *free volume*. **This approximate classical theory is very effective in computations, since it includes thermal expansion** (the response to the spreading pressure exerted by the vibrations), which more sophisticated models ignore. It also does not rely on a harmonic approximation; for these reasons at least, it deserves to be better known.

1.3. SPECIFICITY OF ADSORPTION ON SWCNT AND SWCNT BUNDLES

One of the most interesting issues in adsorption is the basic question of the system dimensionality. A specified nanotube adsorption problem can exhibit behavior characteristic of one, two or three dimensions depending on thermodynamic (temperature and number of particles) or microscopic (atomic size relative to nanotube radius) parameters, and geometry (independent tubes or bundles).

The study of adsorption of atoms on nanotube surfaces is also essential for nano-electronics aiming to achieve low resistance ohmic contacts to nanotubes and to fabricate functional nanodevises. It is important for nanotechnology to produce nanowires with controllable sizes. While the adsorption on the surface of a SWCNT is a two-dimensional process, the diffusion of substances in the tubes is one-dimensional process.

1.3.1. *Adsorption on SWCNT*

It was shown with the help of first-principles gradient-corrected density-functional calculations (Pati et al, 2002) that the adsorption of water molecules on a SWCNT causes a reduction of the electronic conduction due to charge transfer between the adsorbate and the SWCNT: 0.03e is transferred from a single water molecule to the nanotube. The authors conclude a physisorption although they claim a weak bond between a hydrogen atom of a water molecule and one C atom.

A systematic study of single atoms adsorption on a carbon nanotube has been performed by Durgun et al., 2003. Higher coverage and decoration of adsorbed foreign atoms can produce nanostructures such as nanomagnets, nanometer size magnetic domains, one-dimensional conductors and thin

metallic connects, which could be used in technological applications as spintronics and high density data storage. The d-orbitals of the transition metal atoms are responsible for a relatively high binding energy that displays a variation with the number of filled d-states.

The main result of the experimental study of Zhang et al (2000, 2000a) that continuous nanowires of any metal can be obtained by coating the SWCNT with titanium. The strong interaction between Ti and SWCNT can be understood in the frame of density functional theory, which will be described in some detail in the Section 2.1.

The average exchange time between methane molecules adsorbed inside SWCNTs and the free gas outside is estimated to be about 80 ms from nuclear magnetic resonance measurements (Kleinhammes et al 2003).

1.3.2. *Adsorption in bundles of SWCNT*

Experimental results of methane adsorption on closed-ended single-wall nanotube bundles (Talapatra, 2002) give the isosteric heat of adsorption as a function of the amount of methane adsorbed on the SWNT substrate for coverage in the first layer. The isosteric heat of adsorption is found to decrease with increasing coverage. This behavior provides an explanation for differences in previously reported values for this quantity. Substantial agreement was found with previous reports on the temperature dependence of the pressures at which the two first-layer sub-steps occur for methane adsorbed on SWNT bundles.

Grand canonical MonteCarlo simulations with a Lennard-Jones potential have been performed to study the adsorption of methane, X and Ar onto bundles of closed SWCNT (Shi, 2003). The results agree with the experiments of Talapatra, et al., 2002: four different adsorption sites have been identified on bundles of SWCNTs – internal (endohedral), interstitial channels (ICs), external groove sites, and external surfaces. The main conclusion is that the ICs become important in the case of heterogeneous bundles. However, there is no obvious plateau region corresponding to groove site filling for the heterogeneous bundles for methane and Ar and the authors conclude that the groove sites for both homogeneous and heterogeneous bundles are very similar.

The kinetics of adsorption and desorption of methane, Xe, SF6, and other weakly bonded gases from SWCNT bundles has been compared with that from graphite by Hertel (2001). The observed trends in the binding energies of gases with different van der Waals radii suggest that the so-called groove sites on the external bundle surface are the preferred low coverage adsorption sites due to their higher binding energy. The measured sticking coefficients can be related to the diffusion kinetick of adsorbates into the bulk of the nanotube samples.

1.3.3. *Adsorption of methane on graphene*

Methane is of great interest both as a greenhouse gas and as a possible source of hydrogen for fuel cells. A lot of articles have been published on the properties of methane. Our interest in methane has been rooted in the ability of methane to form clathrates or gas hydrates in very cold water under a high pressure. We have re-visited the problem of hydrophobic-molecule influence on liquid and solid water structures (Daykova 2002) in order to understand the competition between the enthalpy and the entropy of clathrate formation. We have suggested a statistical model of the rearrangement of water molecules when methane molecules are introduced in the ideal tetrahedral hydrogen-bond network. The most important basis of that model, which considered the methane molecules as rigid objects, has been the hydrophobic interaction. Methane molecules are less rigid if they interact with carbon atoms.

The electronic structure of graphene, a single planar sheet of sp^2-bonded carbon atoms, provides the basis for understanding the electronic structure of single-walled carbon nanotubes. Recently a lot of efforts have been put into developing applications of SWCNT as gas sensors as the electronic and transport properties of the SWCNTs are significantly changed if they are exposed to gases (Collins 2000). The gas molecules are either physisorbed or chemisorbed depending on the reactivity of the gas.

A microscopic theory of physisorption applied for the noble He atoms on variety of free electron metals showed a little influence of the boundary conditions for a non-local model on the equilibrium distance (Landman 1975). This justifies the study of adsorption of methane (resembling the noble gases in interaction with other atoms) on an isolated piece of graphene sheet.

Extensive time-dependent density-functional calculations (DFT) have been performed (Daykova, 2005) with the real-space DFT code (Chelikowsky, 2000) to study the mechanism of adsorption of methane and to check the influence of the slab finite size on the dynamics of the process and the electron distribution as a result of open 'ends' of the slab. Thus, no boundary conditions have been introduced. The computations without periodic boundary conditions are more demanding. Hence, a preliminary research for the volume and its shape should be done. In the present study a cubic box with a side-length of 17.46 Å has been chosen for the graphene slab with a diameter of 8.98 Å, Figure 1 (a). The grid of calculations is 110 x 110 x 110 with a space-step of 0.3 Bohr = 0.1587 Å; the cut-off radius is 5.29 Å; the time step of electron density integration is 1.2 fs; constant-temperature molecular dynamics (MD) calculations at each time step with a friction-mass of 0.0004 a.u. is used for optimizing the configuration at T=0 K. Under these conditions the electron density at the cut-off radius reduces to 5.4 10^{-9} with a respect to the maximum density. There is no need for

increasing the box size or the cut-off radius. Details of procedure have been published by the code authors (Vassiliev et al. 2002) and (Proykova 2003).

The center of mass of methane molecule is above the point 0 on the graphene sheet, Figure (a), initially at a height of 2.91 Å. The height is optimized with a combined DFT and MD calculations to be 3.07 Å. We have considered two different orientations of the methane molecule relative to the graphene surface. Case 'F', Figure 1 (b), is characterized with a binding energy of 120±10 meV, which shows a physisorption and agrees surprisingly well with previous calculations of Muris et al. (2001) based on a constant-temperature Monte Carlo method. They have found that the binding energy for a single methane molecule is –121±10 meV for the curved graphitic surface; for planar graphite it is –143±10 meV.

The case 'V' denotes a methane molecule rotated at 180° with respect to the position in the Figure 1 (b). In this case one C-H bond is closer to the graphene slab and the other three are further. The binding energy is larger manifesting a configuration dependence reported for Li adsorbed on CNT (Udomvech 2005).

The methane-graphene interaction induces a local curvature of the graphene: in the 'F' case it is hardly seen, Figure 1 (b), while in the 'V' case it is essential.

The oscillations of CH4 center of mass in the Figure 1 (c) reveal a faster dynamics in the 'F' case. This result combined with the smaller adsorption energy in the 'F' case, shows that this case is less stable.

To find out the mechanism of adsorption we study the electron distribution change in both methane and graphene slab due to methane-graphene interaction. Additionally, changes of the fundamental modes of methane bring information about the interaction. We compare our calculations with the experimentally determined values for the fundamental modes of methane obtained by Allan (2005) with the help of electron energy loss spectroscopy, Table 2.

Table 2 Vibrational modes of methane (symmetry Td)

Mode	Sym species	Type	Frequency (meV)	Line width (meV)	Activity
ν1	*A*1	Symmetric stretch	361.7		Raman
ν2	*E*	Twisting	190.2	30	Raman
ν3	*T2*	Asym. stretch	374.3		IR
ν4	*T2*	Scissoring	161.9	16	IR

Note that the outer graphene bonds {lines 3, 4 in the Figure 1, (**e**) and (**f**)} oscillate with a period of ≈11 fs, which is the same as the asymmetric stretch mode 11.05 fs (374.3 meV) of the methane molecule. Summation of the two wave processes cause beating which we see in the dynamics of the electron distribution in the methane molecule.

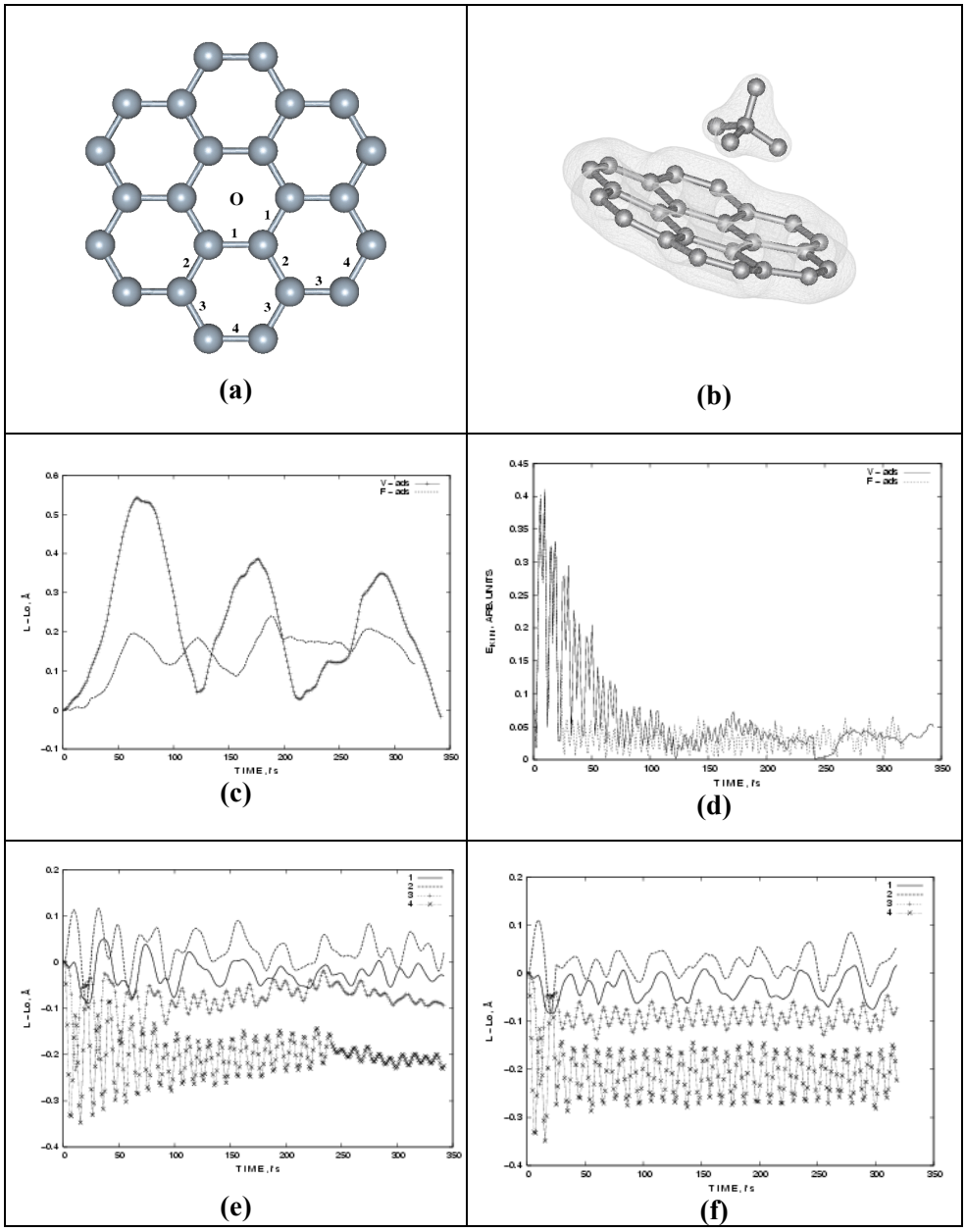

Figure 1 The CH4 molecule is initially at r_0= 2.91 Å above point 0 in the graphene sheet (**a**); 1, 2, 3, and 4 label the bonds between C atoms in the sheet and appear in the figures (**e**) and (**f**); (**b**) the 'F' orientation of CH4; (**c**) the relative amplitude of induced oscillations of the CH4 center of mass for the cases 'F' and 'V',; (**d**) the kinetic energy of the system (molecule & graphene) as a function of time: after 150 fs the temperature is almost 0 K; the oscillations of graphene bonds '1','2','3', and '4' for 300 fs: (**e**) 'V' case; (**f**) 'F' case.

1.4. RELATIONSHIP OF POTENTIAL ENERGY CURVES TO ELECTRONIC SPECTRA OF A DIATOMIC MOLECULE ADSORBED ON A SURFACE

To understand differences in adsorption of various atoms/molecules we inspect the potential energy (Morse) curve, Fig. 2 (**a**), for a diatomic molecule versus the inter-nuclear distance. The minimum and maximum values for the bond distance for the vibrational state are at A and B (see caption to the figure). At those points the atoms change direction, so the *Vibrational Kinetic* energy is zero. At r_e (equilibrium internuclear distance) the *Vibrational Kinetic* energy has a maximum value and the *Vibrational Potential* energy is zero. Each horizontal line represents a vibrational state. The ground state is v_0 and thee excited states are v_1, v_2 ,v_3 etc. Each excited state contains a series of different vibrational energy levels and may be represented by a Morse curve. Each vibrational level v_n is described by a vibrational wave function Ψ_{vib}. The square of wave function gives the probability distribution, and in this case Ψ_{vib}^2 indicates the probable internuclear distance for a particular vibrational state (the dotted line). The higher the line the more probable the internuclear distance is. The most probable distance for a molecule in the ground state is r_e, while there are two probable distances that correspond to the two maxima in the next vibrational state; three in the third, Fig.2 (**b**). In the excited vibrational levels for the ground state and the excited electronic states, there is a high probability of the molecule having an inter-nuclear distance at the ends of the potential function.

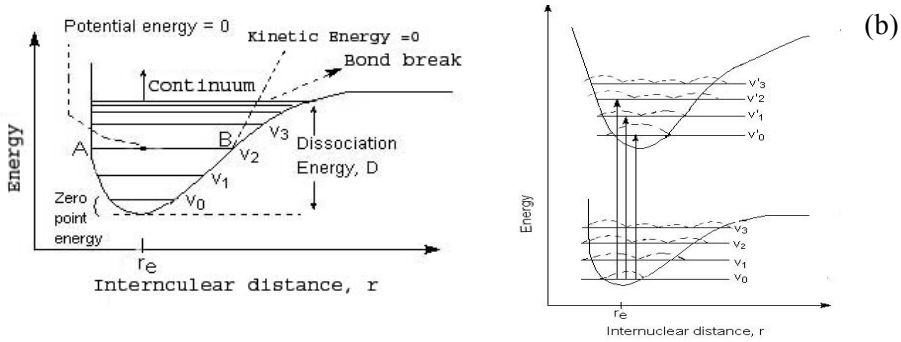

Figure 2 (**a**) Morse curve: Along the A-B line we see that the energy is constant while the bond distance (**b)** is changing, that means the molecule is vibrating , and A-B is a vibrational state.

2. Time-scales in Molecular Dynamics. Ab-initio (quantum) Molecular Dynamics and coarse graining techniques

To determine properties of materials one needs to approximate both atomic and electronic interactions. However, these interactions have completely different time and space scales. Because of the large difference between the masses of electrons and nuclei and the fact that the forces on the particles are the same, the electrons respond instantaneously to the motion of the nuclei. Thus, the nuclei are adiabatically treated and separated from the electrons. The many-body wave function is factorized

$$\Psi(\mathbf{R}_I, \mathbf{r}_n) = \Psi_{el}(\{\mathbf{r}_n\};\{\mathbf{R}_I\})\Psi_l(\{\mathbf{R}_I\})$$

within the Born-Oppenheimer approximation. The adiabatic principle reduces the many-body problem in the solution of the dynamics of the electrons in a frozen-in configuration $\{\mathbf{R}_I\}$of the nuclei. This is an example of how some degrees of freedom are eliminated in the multi-scale modeling.

The structure of matter is continuous when viewed at large length scales and discrete at an atomic scale. Modeling techniques are being developed to bridge the gap between the length-scale extremes. Nanotechnology challenges the researchers to develop and design nanometer to micrometer-sized devices for applications in new generations of computers, electronics, photonics and drug delivery systems. Theory and modeling play more and more important role in these areas to reduce costs and increase predictability for the new properties. Multi-scale materials modeling approaches are required to combine the atomistic and continuum scale. A detailed overview of recent achievements has been completed by Ghoniem and collaborators (Ghoniem et al 2003).

SWCNT is a good example of the dual behavior of the matter. Their functionalization is done at an atomic level (bonding manipulation) while their elastic modulus shows up at the continuous level.

2.1. DENSITY FUNCTIONAL AND MOLECULAR DYNAMICS METHOD

The Car-Parrinello (CP) method was applied to perform both dynamic and static calculations. The method performs the classical MD, which computes a time dependent trajectory of all the atomic motions by numerically integrating equation of motion, and simultaneously applies DFT to describe the electronic structure, using an extended Lagrangian formulation. The characteristic feature of the Car-Parrinello approach is that the electronic wave function, *i.e.* the coefficients of the plane wave basis set, are dynamically optimized to be consistent with the changing positions of the atomic nuclei. The actual implementation involves the numerical integration of the equations of motion of

second-order Newtonian dynamics. A crucial parameter in this scheme is the fictitious mass associated with the dynamics of the electronic degrees of freedom. Nosé (1984) has modified Newtonian dynamics so as to reproduce both the canonical and the isothermal-isobaric probability densities in the phase space of an *N*-body system. Nosé did this by scaling time (with *s)* and distance (with $V^{1/D}$ in *D* dimensions) through Lagrangian equations of motion. The dynamical equations describe the evolution of these two scaling variables and their two conjugate momenta p_s and p_v. In practice, the fictitious mass has to be chosen small enough to ensure fast wave function adaptation to the changing nuclear positions on one hand and sufficiently large to have a workable large time step on the other. In our work (Daykov and Proykova 2001) the equations of motion were usually integrated using the Verlet algorithm (Verlet 1967). The fictitious mass limits the time step.

The CP simulations can be performed using the CP-PAW code package developed by Blöchl (1994). It implements the ab-initio (from first-principles) molecular dynamics together with the **projector augmented wave** (PAW) method. The PAW method uses an augmented plane wave basis for the electronic valence wave functions, and, in the current implementation, frozen atomic wave functions for the core states. Thus it is able to produce the correct wave function and densities also close to the nucleus, including the correct nodal structure of the wave functions. The advantages compared to the pseudopotential approach are that transferability problems are largely avoided, that quantities such as hyperfine parameters and electric field gradients are obtained with high accuracy (Petrilli et al., 1998; Blöchl 2000) and, most important for the present study, that a smaller basis set as compared to traditional norm-conserving *pseudopotentials* is required.

It is well known that most physical properties of solids are dependent on the valence electrons to a much greater degree than that of the tightly bound core electrons. It is for this reason that the *pseudopotential* approximation is introduced. This approximation uses this fact to remove the core electrons and the strong nuclear potential and replace them with a weaker pseudopotential which acts on a set of pseudo wavefunctions rather than the true valence wavefunctions. In fact, the pseudopotential can be optimised so that, in practice, it is even weaker than the *frozen core potential* (Lin et al 1993).

The frozen core approximation was applied for the 1s electrons of C and O, and up to 2p for Cl. For H, C and O, one projector function per angular-momentum quantum number was used for **s**- and **p**-angular momenta. For Cl, two projector functions were used for **s**-and one for **p**-angular momenta. The Kohn-Sham (Kohn and Sham 1965) orbitals of the valence electrons were expanded in plane waves up to a kinetic energy cutoff of 30 Ry.

Static DFT calculations can be performed using the atomic-orbital based ADF package (Baerends et al., 1973). In these calculations, the Kohn-Sham orbitals were expanded in an uncontracted triple-Slater-type basis set augmented with one 2p and one 3d polarization function for H, 3d and 4f polarization functions for C, O, and Cl.

For heavy atoms, relativistic effects become important because electrons near the nuclei move at speeds that are a significant fraction of the speed of light. The electron wave functions near the nuclei must therefore be described by the Dirac equation. However, the pseudopotential method can also be applied here. To determine the radial wave functions, one must work with a generalization of the radial Kohn-Sham equations that correspond to the Dirac equation. The steps in creating a pseudopotential are now modified as follows: Step 1 - one must write down and solve a version of the Kohn-Sham equations that generalizes the Dirac equation; Step 2 - one draws smooth replacements for the original wiggly wave functions. One can take the original nonrelativistic Kohn-Sham equation and put a pseudopotential in it that produces the wave functions obtained in the previous step. Now the pseudopotential is not only compensating for the smoothing procedure of step 2 that removed wiggles from the wave function, but also is compensating for the differences between the Dirac equation and the Schroedinger equation. That is, the pseudopotential is chosen to produce a wave function for the Schroedinger equation that is also a solution of the original Dirac equation.

DFT and MD methods have been simultaneously applied to study conductivity and mechanical properties of (10,0) SWCNT (Iliev et al, 2005). Molecular dynamics simulations have shown that the distribution of the vacancies, not only their concentration, is important for the mechanical strength of the tube. Our calculations demonstrate that the band gap shrinks in a defective tube and the external field changes the band gap differently depending on the axis of application.

Insight of carbon nanotube growth has been gained from DFT and tight binding studies (Krasheninnikov et al 2004). They have found that the adsorption and migration energies strongly depend on the nanotube diameter and chirality, which makes the model of carbon adatom on a flat graphene sheet inappropriate. This result is consistent with our finding (Daykova et al 2005) that adsorption of methane on a small graphene sheet induces curvature of the sheet, which is not flat anymore. Krasheninnikov and collaborators have used the PAW method to describe the core electrons and the generalized gradient approximation (Perdew and Wang 1992, Perdew et al 1992). They have found that adatom migration is a different mechanism from the kick-out mechanism as it was previously derived from analytical potential calculations (Maiti1967).

2.2. SPACE-TIME DISCRETE POINTES

For the numerical solution of time-dependent wave propagation problems that appear both in DFT and *ab initio* MD one has to deal with complex geometries with very different evolution scales. The time step of the computations is determined by the fastest process in order to predict reliable results. For a comparison, the electronic degrees of freedom should be integrated in the atto-second domain, while the nuclear degrees of freedom are in the femto-second domain. If a uniform time-step (fastest process) Δt is used two problems appear. First, the computational cost is high. Second, the ratio $c\Delta t/(space\_step)$ in the coarser grid will be much smaller than its optimal value. This generates dispersion errors in most numerical schemes. To avoid these problems, it is advisable to keep the ratio constant meaning that Δt is different in the various space domains determined by the density distribution of the original system. The Figure 3 shows replacement of a uniform time-space mesh with a refined mesh for a complex structure, which is much denser in the middle of the area than at the boarders. At different time-steps (they could be very different) one can use various space discrete steps.

The mesh refinement is an opposite approach to coarse-graining techniques, which we will consider in the next section. At the end of the present section we must underline that the use of local time step raises new practical and theoretical problems that are very delicate in the case of hyperbolic equations. There are plenty of articles on the subject, see for example (Manfrin 1996) and the references there in.

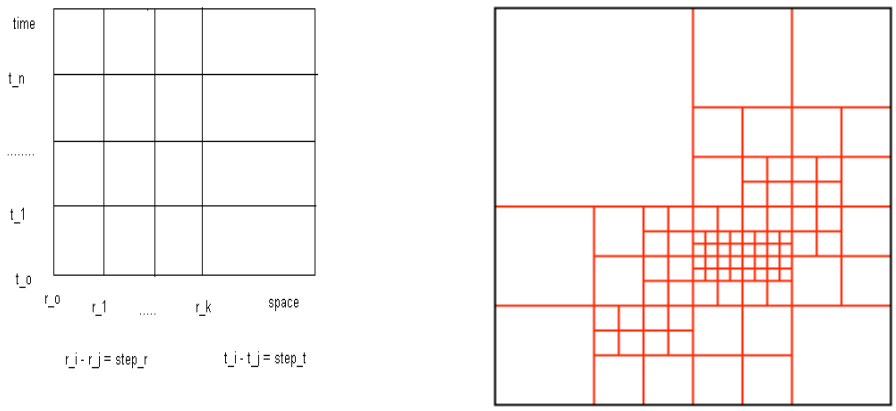

Figure 3 The uniform time-space mesh (left) is replaced by a suitable dynamic mesh.

2.3. COARSE-GRAINING TECHNIQUE: TIME/TEMPERATURE DEPENDENT PHENOMENA

The study of time/temperature dependent phenomena is more difficult and requires the development of a dynamics for a system with an inhomogeneous level of coarse graining. A nice job has been completed by Stefano Curtarolo in his dissertation for the degree of PhD in material science (Curtarolo 2003). The technique suggested is different from both microscopic (quantum mechanics) and macroscopic (thermodynamics) descriptions. By removing the unnecessary degrees of freedom, the author constructs a local thermodynamics associated with dynamics and interaction between regions.

An example useful for the carbon nanotubes is the following. Let us consider a finite one dimensional chain of atoms that interact through nearest neighbor pair potentials. It is possible to remove every second atom by considering each of these atoms as part of a local system with its own local partition function. The local degrees of freedom can be removed by integrating over all the possible configurations of the particular atom. The integration produces a local partition function, local free energy and local entropy, which equals the information that has been locally removed from the system. This construction 'converts' the second neighbors into first neighbors with an effective potential which is the microscopic analogy of the pressure for thermodynamic systems. The procedure can be iterated until a multi-scale description of the systems is achieved. This approach is rigorously correct at equilibrium being an approximate one to slow dynamics description.

Coarse graining requires both a scheme to remove atoms and a recipe for constructing potentials between the remaining atoms. One way is the integration of bond motion similarly to the Migdal-Kadanoff approach in renormalization group theory (Migdal 1975, Kadanoff 1976, Kadanoff 1977). New potentials can be differently defined satisfying the requirements: a) the coarse-grained system ultimately evolves to the same equilibrium state of the atomistic one; b) the information removed from the original system is quantified by the entropy contribution of each coarse graining. Curtarolo has used as a criterion for the definition of a new potential: the partition function should be unchanged in the coarse graining procedure.

3. Diffusion of the adsorbed gases

An important observation has been that adsorbed atoms (adatoms) form small clusters which diffuse on metal surfaces by undergoing possible cluster configurations. The nature of the motion depends on the surface morphology.

Examples are one-dimensional diffusion of W on the (211) W surface and two-dimensional diffusion of Pt on W. What is the dimensionality of gas diffusion on/in nanotubes?

Different approaches – experimental, computational, and theoretical – give supplementary information on the specific features of particle diffusion on/in CNT and SWCNT bundles.

Theoretically one solves the generic diffusion equation

$$\partial c / \partial t - \nabla.(D\nabla c) = Q,$$

where $c = N_a/A$ is the concentration of the ad-atoms, D is the diffusion coefficient and Q is a volume source, may be anisotropic in which case D is a 2-by-2 matrix. The boundary conditions can be of Dirichlet type, where the concentration on the boundary is specified, or of Neumann type, where the flux n.(D∇(c)) is specified. It is also possible to specify a generalized Neumann condition. It is defined by n. (D∇(c)) + qc = g, where q is a transfer coefficient. This approach does not reflect the discrete nature of SWCNTs, which restricts its applications.

Recent research reveals that binary gases and fluids diffuse differently at the nano-scale than many other polyatomic molecules. For example, *n*-butane and isobutene are predicted to have substantially different separation behaviors when they are mixed with methane molecules in a single-wall carbon tube (Moe, 2001). Further studies to determine the exact mechanisms responsible for this unique trait are, however, a great challenge due to the difficulty of detecting and determining the behavior of the molecules experimentally.

Atomistic simulations (Skoulidas et al 2002) for both self- and transport diffusivities of methane and hydrogen in CNT predict orders of magnitude faster transport than that in zeolites. The high rates in CNT result from the inherent smoothness of the nanotubes. The authors used equilibrium dynamics to obtain the diffusion coefficients.

There is an interest in Li adsorption and diffusion on/in CNT in relation with Li batteries production. Frontera and collaborators (Garao et al 2003) studied molecular interaction potential between Li^+ and small-diameter arm-chair SWCNT based on ab initio calculations. They observed a channel that would allow ion mobility inside the nanotube. Since the Li atom and cation prefer to localize near the carbon nanotube sidewall, small-diameter carbon nanotubes are more advantageous than the larger ones for batteries usage.

The rate of diffusion is inversely related to the binding energy. Density functional computations based on the B3LYP functional and all-electron basis set centered on atoms show that the binding energy depends on the configuration rather than on the diameter size (Udomvech et al 2005). This

result contradicts the finding of Krasheninnikov and thus needs an independent study.

To complete this section it is important to note that the diffusion process is the basis of various phenomena icluding carbon nanotube growth by carbon diffusion; convey of nanoscale materials with the help of SWCNT; migration of defects; gas separation and filtration.

One of the future challenges is the development of explicit links between the atomistic scales and the continuum level in all numeric techniques included in the present paper. The issue of computational efficiency must be also addressed so that truly large-scale simulations on thousands of processors can be effectively performed.

Acknowledgements: Computations on the methane adsorption on graphene has been performed with a partial support from HPC-Europe (CINECA.Italy). The results for the influence of external electric field on defective SWCNT have been calculated under the Taiwan-Bulgarian project. A Grant from the Ministry of Education and Science (У-Ф-03/03) and a grant from the University of Sofia (2005) have been used for calculations of mechanical strength of carbon nanotubes.

References:

Allan, M., 2005, Excitation of the four fundamental vibrations of CH4 by electron impact near threshold, *J. Phys. B: At. Mol. Opt. Phys.* **38**: 1679-1685.

Baerends, E.J.; Ellis, D.E.; and Ros, P., 1973, Self-consistent molecular Hartree—Fock—Slater calculations I. The computational procedure**,** *Chem. Phys.* **2**:41-51.

Bienfait, M., Zeppenfeld, P., Dupont-Pavlovsky, N., Muris, M.R., Wilson, T., DePies, M., and Vilches, O.E., 2004, Thermodynamics and structure of hydrogen, methane, argon, oxygen, and carbon dioxide adsorbed on sigle wall carbon naotube bundles, *Phys. Rev. B* **70** : 035410

Blöchl, P.E., 1994, Projector augmented-wave method, *Phys. Rev. B* **50**: 17953-1797.

Blöchl, P.E., 2000, First-principles calculations of defects in oxygen-deficient silica exposed to hydrogen *Phys. Rev. B* **62**: 6158-6179.

Car, R., Parrinello, M., 1985, Unified approach for Molecular Dynamics and Density-Functional Theory, *Phys. Rev. Lett.* **55**: 2471-2474.

Chelikowsky, J. R., 2000, The pseudopotential-density functional method applied to nanostructures, *J. Phys. D: Appl. Phys*. **33**: R33-R50 http://jrc.cems.umn.edu/codes.htm

Collins, P.G., Bradley K., Ishigami, M., and Zettl., A., 2000, Extreme Oxygen Sensitivity of electron properties of carbon nanotubes, *Science* **287:** 1801-1804.

Curtarolo, Stefano, 2003, Coarse-Graining and Data Mining Approaches to the prediction of structures and their dynamics, Ph.D. thesis, MIT (USA).

Daykov, I., and Proykova, A., 2001, Cluster size dependence of the temperature interval of coexisting phases observed in plastic molecular clusters, in *Meetings in Physics at University of Sofia*, A. Proykova, ed. , **v.2**, Heron Press Science Series, Sofia, pp. 31-35.

Daykova, E., Pisov, S., and Proykova, A., 2005, First-principles and molecular dynamics simulations of methane adsorption on graphene, **NATO ASI** vol.

Daykova, E. , Proykova, A., and Ohmine, I., 2002, Statistical Calculations of Entropy of Methane Clathrate, in *Meetings in Physics @ University of Sofia* **3**: 44 -48

Durgun, E., Dag, S., Bagci, V.M.K., Gulseren, O., Yildirim, T., and Ciraci, S., 2003, Systematic study of adsorption of single atoms on a carbon nanotube, *Phys. Rev. B* **67**:201401.

Garao, C., Frontera, A., Quinonero, D., Costa, A., Ballester, P., Deya, P.M., 2003, Lithium diffusion in single-walled carbon nanotubes: a theoretical study, *Chem. Phys. Lett.* **374:**548.

Ghoniem, N., Busso, E., Kiossis, N., and Huang, H., 2003, Multiscale modeling of nanomechanics and micromechanics: an overview, *Philosophical Magazine* **83:** 3475-3528.

Hertel, T., Kriebel, J., Moos, G., and Fasel, R., 2001, Adsorption and desorption of weakly bonded adsorbates from single-wall carbon nanotube bundles, AIP Conference Proceedings 590, „Nanonetwork Materials, Fullerenes, Nanotubes and Related Systems“, (Kamakura, Japan, ed. by S. Saito, T. Ando, Y. Iwasa, K. Kikuchi, M. Kobayashi, Y. Saito) p.181

Hill, T.L., 1987, *Statistical Mechanics: Principles and Selected Applications*, Dover, New York.

Hill, T. L., 1986, *An Introduction to Statistical Thermodynamic,*.Dover, New York.

Hill, T.L., 1994, *Thermodynamics of Small Systems*, Parts I and II, Two Volumes in One. Dover, New York.

Iliev, H., and Proykova, A., 2004, Mechanically induced defects in single-wall carbon nanotubes, in *Meetings in Physics at University of Sofia*, A. Proykova, ed., **v.5**, Heron Press Science Series, Sofia, pp.87-91.

Iliev, H., Li, F.-Yin, and Proykova, A., 2005, Carbon nanotubes with vacancies under external mechanical stress and electric field, **NATO ASI** vol.

Kadanoff, L. P. , 1976, Notes on Migdal's Recursion Formulas, *Ann. Phys.* **100:**359

Kadanoff, L. P., 1977, The Application of Renormalization Group Techniques to Quarks and Strings, *Rev. Mod. Phys.* **49**: 267

Kleinhammes, A., Mao, S.-H., Yang, X.-J., Tang, X.-P, Shimoda, H., Lu, J.P., Zhou, O., and Wu, Y., 2003, Gas adsorption in single-walled carbon nanotubes studied by NMR, *Phys. Rev.* ***B*** **68**: 075418 (6 pages).

Kong, J., Franklin, N.R., Zhou, C., Chapiline, Peng, S., Cho, K., and Dai, H., 2000, Nanotube Molecular Wires as Chemical Sensors, *Science* **287**: 622-625

Kohn, W. and Sham, L.J., 1965, Self-consistent equations including exchange and correlation effects, *Phys. Rev.* **140:** A1133-A1138**.**

Krasheninnikov, A.V., Nordlund, K., Lehtinen, P.O., Foster, A.S., Ayuela, A., and Nieminen, R.M., 2004, Adsorption and migration of carbon adatoms on carbon nanotubes: Density-functional *ab initio* and tight-binding studies, *Phys. Rev.* B **69**: 073402 (4 pages).

Landman, Uzi and Kleinman, George, 1975, Local and non-local effects in the theory of physisorption, *J. Vac. Sci. Technol.* **12**: 206-209.

Lin, J. S. , Qteish, A., Payne, M. C. and Heine, V., 1993, Optimized and transferable nonlocal separable *ab initio* pseudopotentials, *Phys. Rev. B*, **47:** 4174-4180.

Maiti, A., Brabec, C.J., and Bernholc, J., 1997, Kinetics of metal-catalyzed growth of single-walled carbon nanotubes, *Phys.Rev.* B **55:**R6097-R6100.

Manfrin, R. (1996) On the gevrey regularity for weakly hyperbolic equations with space-time degeneration of oleinik type, *Rendiconti di Matematica* **16:** 203-231.

Migdal, A.A., 1975, *Zh.Eksp. Teor. Fiz.* **69**:1457.

Moe, Zugang and Susan B. Sinnott, 2001, *Separation of Organic Molecular Mixtures in Carbon Nanotubes and Bundles: Molecular Dynamics Simulations*, The University of Kentucky, 177 Anderson Hall, Lexington, Kentucky 40506-0046.

Muris, M., Bienfait, M., Zeppenfeld, P., Dupont-Pavlovsky N., Wass, P., Johnsons, M., Vilches, O.E., and Wilson, T., 2001, http://www.ill.fr/AR-01/p-82.htm and references there in

Nosé, S.J., 1984, Constant temperature molecular dynamics methods, *J. Chem. Phys.* **81**: 511-519.

Pati, R., Zhang, Y., and Nayak, S., 2002, Effect of H2O adsorption on electron transport in a carbon nanotube, *Appl. Phys. Lett.* **81**: 2638-2640.

Perdew, J. and Wang Y., 1992, Accurate and simple analytic representation of the electron-gas correlation energy, *Phys. Rev.* B **45:** 13244-13249.

Perdew, J.P., Chevary, J.A., Vosko, S.H., Jackson, K.A. Pederson, M.R., Singh, D.J., and Fiolhais, C., 1992, Atoms, molecules, solids, and surfaces: Applications of generalized gradient approximation for exchange and correlation, *Phys.Rev.* B **46:**6671-6687.

Petrilli, H.M.; Blöchl, P.E.; Blaha, P.; Schwarz, K., 1998, Electric-field-gradient calculations using the projector augmented wave method, *Phys. Rev. B* **57**: 14690-14697.

Proykova, A., Pisov, S., Radev, R., Mihailov, P., Daykov, I., and R.S.Berry, 2001, Dynamical Phase Coexistence of Molecular Nano-clusters: Kinetics versus Thermodynamics, in *Nanoscience&Nanotechnolgy*, E. Balabanova and I. Dragieva, eds. pp.18-20, Heron Press Science Series, Sofia.

Proykova, A., 2002, The role of metastable states in the temperature driven phase changes of molecular nano-clusters*, Vacuum* **68**:.97-104.

Proykova, A., Pisov, S., Dragieva, I., and Chelikowski, J., 2003, DFT Calculations of optimized structures of some coordination compounds, *Nanoscience&Nanotechnolgy'03*, E. Balabanova and I. Dragieva, eds., Heron Press Science Series, Sofia.

Proykova, A., and Iliev, H., Simulated stress and stretch of SWCNT, in *Proceedings of SIMS 2004*, pp. 273-279, Brian Elmegaard, Jon Sporring, Kenny Erleben, Kim Sorensen eds., Copenhagen.

Shi, Wei and Johnson, J. Karl, 2003, Gas adsorption on Heterogeneous Single-Walled Carbon Nanotube Bundles, *Phys. Rev. Lett.* **91**:015504-1.

Skoulidas, A., Ackerman, D., Johnson, J.K., and Sholl, D., 2002, Rapid transport of gases in carbon nanotubes, *Phys. Rev. Lett.* **89**:185901 (4 pages).

Spurling, T.H., De Rocco, A.G., and Storvick, T.S., 1968, Intermolecular Forces in Globular Molecules. VI. Octopole Moments of Tetrahedral Molecules, *J. Chem. Phys. J. Chem. Phys.* **48:** 1006-1008.

Talapatra, S. and Migone, A.D., 2002, Adsorption of methane on bundles of closed-ended single-wall carbon nanotubes, *Phys. Rev.* B **65**: 045416 (6 pages).

Udomvech, A., Kerdcharoen, T., Osotchan, T., 2005, First principles study of Li and Li+ adsorbed on carbon nanotube: Variation of tubule diameter and length, *Chem. Phys. Lett.* **406:**161-166.

Vassiliev, I., Ogut, S., and Chelikowsky, J.R., 2002, First-principles density-functional calculations for optical spectra of clusters and nanocrystals, *Phys. Rev.* B **65**:115416-(1-18)

Venables, John A., 2000, *Introduction to Surface and Thin Film Processes*, Cambridge University Press

Verlet, L., 1967, Computer "experiments" on classical fluids. I. Thermodynamical properties of Lennard-Jones molecules, *Phys. Rev.* **159**: 98-103.

Zhang, Y. and Dai, H., 2000, Formation of metal nanowires on suspended single-wall carbon nanotubes, *Appl. Phys. Let*. **77**: 3015-3017.

Zhang, Y., Franklin, N.W., Chen, R.J., and Dai, H., 2000a, Metal coating on suspended carbon nanotubes and its implication to metal-tube interaction, *Chem.Phys. Lett*. **331**: 35.